# Mode-of-action profiling reveals glutamine synthetase as a collateral metabolic vulnerability of *M. tuberculosis* to bedaquiline

Zhe Wang[a], Vijay Soni[a], Gwendolyn Marriner[b], Takushi Kaneko[c], Helena I. M. Boshoff[b], Clifton E. Barry III[b], and Kyu Y. Rhee[a,1]

[a]Division of Infectious Diseases, Weill Department of Medicine, Weill Cornell Medical College, New York, NY 10065; [b]Tuberculosis Research Section, Laboratory of Clinical Infectious Diseases, National Institute of Allergy and Infectious Diseases, National Institutes of Health, Bethesda, MD 20892; and [c]Global Alliance for TB Drug Development, New York, NY 10005

Edited by William R. Jacobs Jr., Albert Einstein College of Medicine, Bronx, NY, and approved August 19, 2019 (received for review May 14, 2019)

**Combination chemotherapy can increase treatment efficacy and suppress drug resistance. Knowledge of how to engineer rational, mechanism-based drug combinations, however, remains lacking. Although studies of drug activity have historically focused on the primary drug–target interaction, growing evidence has emphasized the importance of the subsequent consequences of this interaction. Bedaquiline (BDQ) is the first new drug for tuberculosis (TB) approved in more than 40 y, and a species-selective inhibitor of the *Mycobacterium tuberculosis* (Mtb) ATP synthase. Curiously, BDQ-mediated killing of Mtb lags significantly behind its inhibition of ATP synthase, indicating a mode of action more complex than the isolated reduction of ATP pools. Here, we report that BDQ-mediated inhibition of Mtb's ATP synthase triggers a complex metabolic response indicative of a specific hierarchy of ATP-dependent reactions. We identify glutamine synthetase (GS) as an enzyme whose activity is most responsive to changes in ATP levels. Chemical supplementation with exogenous glutamine failed to affect BDQ's antimycobacterial activity. However, further inhibition of Mtb's GS synergized with and accelerated the onset of BDQ-mediated killing, identifying Mtb's glutamine synthetase as a collateral, rather than directly antimycobacterial, metabolic vulnerability of BDQ. These findings reveal a previously unappreciated physiologic specificity of ATP and a facet of mode-of-action biology we term collateral vulnerability, knowledge of which has the potential to inform the development of rational, mechanism-based drug combinations.**

metabolomics | mode-of-action | antibiotics | drug combination | tuberculosis

Growing concern about antibiotic resistance and the faltering pipeline of new antibiotics have fueled renewed interest in combination chemotherapies for their ability to increase treatment efficacy and reduce rates of drug toxicity and resistance. However, the development of such drug combinations remains largely empiric (1). Traditional drug development has focused on exploiting the primary drug–target interaction (2, 3). Yet, recent work has begun to emphasize the functional importance of specific secondary or downstream consequences that follow this interaction and mediate drug activity, sometimes referred to as drug mode of action (MoA) (4–8).

Among modern infectious diseases, the importance of combination chemotherapies is established perhaps nowhere more clearly than for tuberculosis (TB). Once associated with mortality rates of as high as 50%, TB was transformed into a predictably curable disease with the advent of antibiotics. This success was achieved only after the introduction of drug combinations that were prompted by early recognition of treatment relapse and secondary drug resistance after monotherapy. Unfortunately, while therapeutically effective, TB chemotherapies remain longer and more complex than for virtually any other bacterial infection, giving rise to unwanted rates of treatment failure, continued transmission, and the emergence of drug resistance (2, 3).

Bedaquiline (BDQ) is a species-selective inhibitor of the c and ε subunits of the *Mycobacterium tuberculosis* (Mtb) ATP synthase and first new TB drug approved in more than 40 y (9–11). BDQ exhibits bactericidal activity against Mtb in vitro, in mouse models of pulmonary TB, and in patients when given for either 2 or 6 mo in combination with a background regimen with multidrug-resistant TB (9, 12). On this basis, BDQ was approved by the US Food and Drug Administration for the treatment of pulmonary multidrug-resistant TB as part of combination therapy in adults (13). Unfortunately, this approval was accompanied by a black box warning because of concerns about potential cardiac toxicities, while reports of clinical resistance to BDQ followed soon after (14).

Here, we characterize the downstream secondary consequences of BDQ-mediated inhibition of the Mtb ATP synthase. We show that despite the hundreds of annotated ATP-dependent metabolic reactions in the cell, treatment of Mtb with BDQ has a preferential indirect secondary effect on glutamine biosynthesis, and that this effect can be exploited to increase the potency of BDQ when combined with an inhibitor of Mtb's glutamine synthetases. These studies thus reveal a previously underrecognized facet of MoA biology with the potential to inform the development of rational, drug-specific combination therapies.

## Significance

**Drug combinations are an important strategy to increase treatment efficacy, reduce drug toxicity, and suppress drug resistance. Their development, however, is often empirical. Here, we report how the secondary consequences of the drug–target interaction (mode of action) can inform the development of rational mechanism-based combinations. We focus on bedaquiline (BDQ), the newest tuberculosis drug, because of known toxicities and emerging reports of resistance. We demonstrate that in addition to inhibiting its primary target, ATP synthase, BDQ causes a secondary inhibition of glutamine biosynthesis that is not directly antimycobacterial but renders *Mycobacterium tuberculosis* hypersensitive to inhibitors of its glutamine synthetase. These studies reveal drug-induced fitness costs as a specific and potentially valuable, but underappreciated, window to rational, mechanism-based drug combinations.**

Author contributions: Z.W. and K.Y.R. designed research; Z.W., V.S., and K.Y.R. performed research; Z.W., G.M., T.K., H.I.M.B., C.E.B., and K.Y.R. contributed new reagents/analytic tools; Z.W., V.S., and K.Y.R. analyzed data; and Z.W. and K.Y.R. wrote the paper.

The authors declare no conflict of interest.

This article is a PNAS Direct Submission.



[1]To whom correspondence may be addressed. Email: kyr9001@med.cornell.edu.

This article contains supporting information online at www.pnas.org/lookup/suppl/doi:10.1073/pnas.1907946116/-/DCSupplemental.

First published September 9, 2019.

## Results

**Identification of Activity-Specific Metabolic Effects of BDQ.** Although potent, BDQ is widely recognized for a characteristic lag in onset of bactericidal activity, with little to no effect on bacterial viability during the first 1 to 2 d at concentrations up to 300× minimum inhibitory concentration (MIC) (15). This lag has been ascribed to the activity of adaptive mechanisms that enable Mtb to persist in slowed or arrested states of replication, where its ATP levels can decrease as much as 90% (16–18). We made use of this lag as an experimental window into the prelethal metabolic consequences of BDQ-mediated inhibition of Mtb's ATP synthase. Using our previously characterized filter culture system and metabolomic profiling platform, we first demonstrated that BDQ readily accumulated in a time- and concentration-dependent manner (*SI Appendix*, Fig. S1), and that this accumulation was associated with a reduction in ATP levels and energy charge, consistent with its known biochemical inhibition of Mtb's ATP synthase (15, 19). This reduction began at ~7.5× MIC and led to a maximum 2-fold decrease of ATP levels at 100× MIC (Fig. 1 *A* and *B* and *SI Appendix*, Figs. S2 and S3). We further demonstrated that these effects occurred before the onset of any measurable effect on Mtb viability, indicative of an antimycobacterial MoA more complex than an isolated reduction in ATP levels (*SI Appendix*, Fig. S4).

To gain further insight into BDQ's antimycobacterial MoA, we next characterized the effect of BDQ versus an inactive enantiomer (BDQi) on the levels of 130 endogenous Mtb metabolites spanning a diverse range of annotated metabolic pathways during this prelethal phase of drug activity (Fig. 1 *C*–*H* and *SI Appendix*, Figs. S2 and S5–S7) (20). This analysis revealed a highly similar pattern of time- and concentration-dependent effects (*SI Appendix*, Fig. S8) that, after a fixed exposure time, consisted in 3 forms of activity-specific response: a monophasic decrease (designated as G1 and G2 in Fig. 1*H*), a monophasic increase (designated as G4),

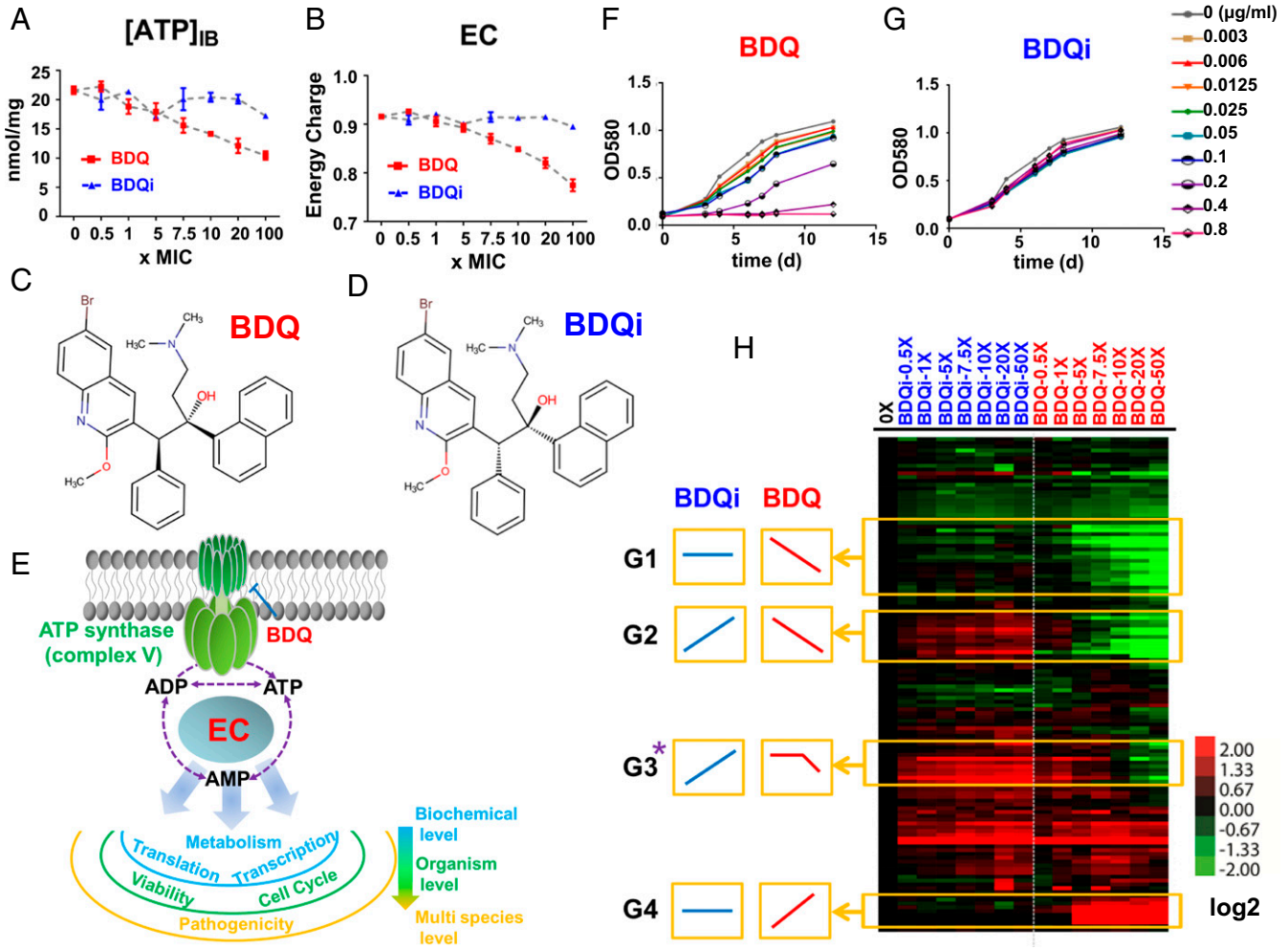


**Fig. 1.** Identification of activity-specific metabolic effects of BDQ. (*A*) Intrabacterial ATP pool sizes, expressed as nanomoles per milligram residual peptide (*y* axis), after exposure of Mtb to a dose range of BDQ (the active diastereomer) spanning 0–100× MIC or equimolar range of BDQi (the inactive enantiomer) concentrations. (*B*) Effect of BDQ and BDQi on calculated energy charge (EC) after exposure of Mtb to the same range of BDQ or BDQi concentrations as in *A*. (*C* and *D*) Stereochemical structures of BDQ and BDQi. (*E*) Schematic of BDQ-mediated inhibition of the Mtb ATP synthase and secondary effect on adenylate (AXP) species (ATP, ADP, and AMP) and EC. (*F* and *G*) Growth curves of Mtb strain H37Rv in the absence and presence of varying concentrations of BDQ or BDQi in 7H9 liquid medium. (*H*) Heat map profile depicting the relative levels of 130 metabolites after 24 h exposure of Mtb to BDQ or BDQi concentrations, as indicated. Columns represent individual treatments as indicated. Rows denote individual metabolites measured. Data were parsed by uncentered Pearson's correlation with centroid linkage clustering and rendered using the image generation program Java TreeView (http://jtreeview.sourceforge.net/). Data are depicted on a $\log_2$ scale relative to untreated control for each compound. G1, G2, G3, and G4 represent metabolite subgroups exhibiting BDQ-specific, but not BDQi-specific, responses, and are designated activity-specific metabolites. Among them, G3-typed metabolites (starred) show the similar changed kinetics with the EC's curve. All data points shown in this figure represent the average of 3 technical replicates and are representative of 2 independent experiments.

and a biphasic or threshold-based decrease (designated as G3; Fig. 1*H*). Moreover, a bio-informatic analysis of these activity-specific responses, performed within the context of all annotated adenylate nucleotide (AXP)-dependent pathways, revealed a statistically significant overrepresentation of metabolites involved in purine, glutamine, CoA, pentose phosphate, and ribose metabolic pathways (*SI Appendix*, Fig. S9 and Tables S1–S4).

**Metabolic Linkage Analysis of BDQ-Associated Activity-Specific Metabolites.** To identify more specific determinants of BDQ activity, we built a metabolic correlation network using the levels of activity-specific metabolites identified here, as well as adenylate nucleotides, ATP, ADP, and AMP, observed in Mtb after both dose- and time-dependent exposures to BDQ. As shown in Fig. 2 *A–C* and *SI Appendix*, Table S5, Pearson correlation analysis identified glutamine as the metabolite most strongly positively correlated with ATP ($r = 0.809$), levels of which serve as an established biochemical surrogate of BDQ's antimycobacterial activity (15).

Given our interest in BDQ's notable lag in bactericidal activity, we focused our attention on glutamine because of its biphasic response to BDQ treatment and strong correlation with ATP levels. Previous work reported that BDQ activity, as reported by MIC, varied according to carbon source (15). We confirmed this finding, noting parallel changes in ATP and glutamine levels that varied with the degree of carbon source-dependent shifts in BDQ potency (*SI Appendix*, Fig. S10).

Glutamine levels in Mtb are primarily determined by the activity of its glutamine synthetases, which catalyze the ATP-dependent assimilation of ammonia into glutamate and in *Escherichia coli* account for ∼15% of its total ATP requirement (21–23). Mtb encodes 4 annotated glutamine synthetase (GS) genes (*glnA1-4*). GlnA1 constitutes the dominant source of detectable activity in cell lysates, and is the only isoform essential for in vitro and in vivo growth (22, 24). We therefore reconstituted the activity of GlnA1 in vitro (*SI Appendix*, Figs. S11 and S12) and characterized its sensitivity to changes in AXP-defined energy charge ratios, similar to those observed after a prelethal 1-d exposure of intact Mtb to antimycobacterial concentrations of BDQ (25). As shown in Fig. 2*D* and *SI Appendix*, Fig. S13, the in vitro activity of GlnA1 decreased over the same range of AXP

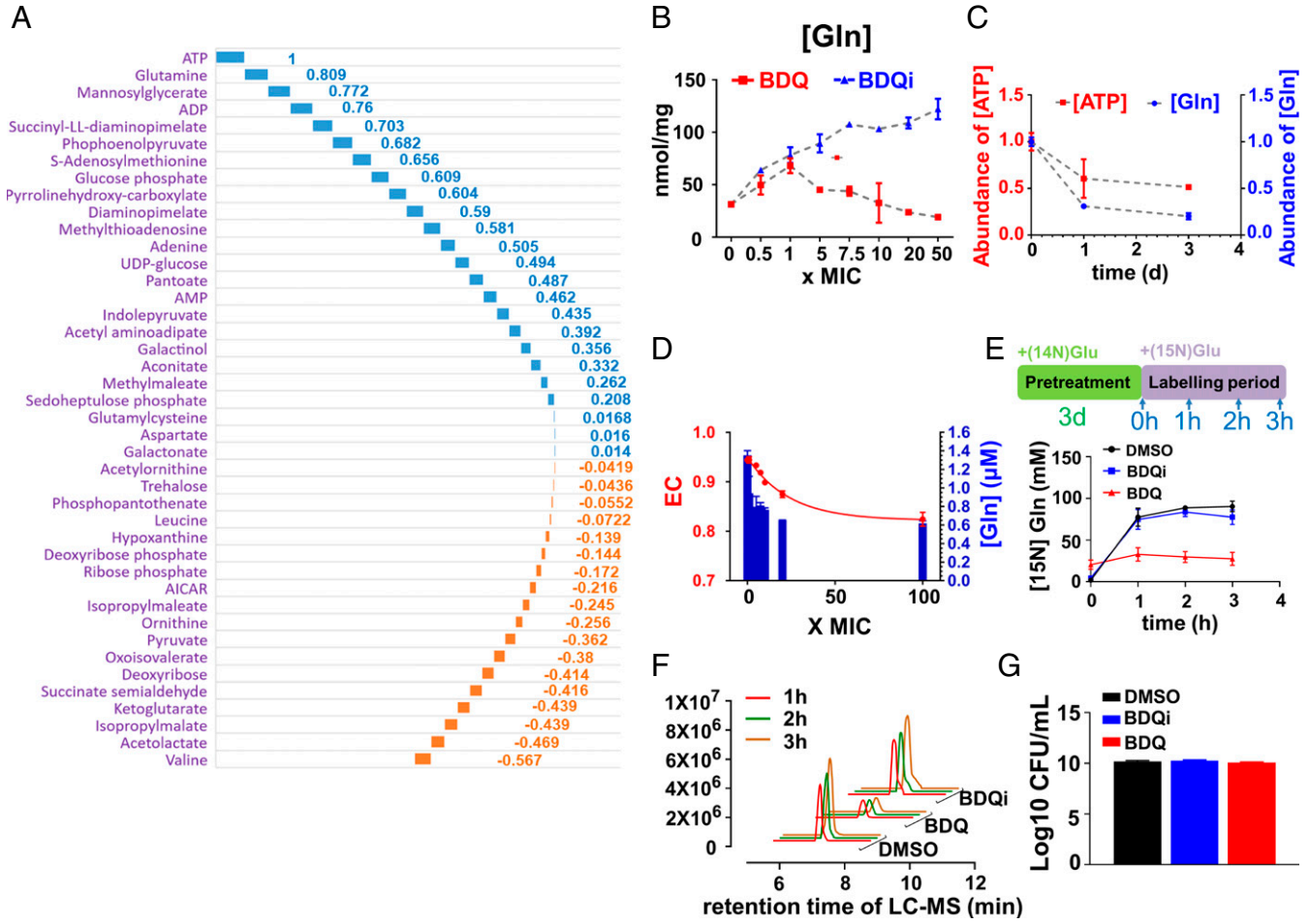


**Fig. 2.** BDQ-specific linkage of ATP and glutamine levels in Mtb. (*A*) Waterfall plot representation of metabolic correlation network between ATP and BDQ activity-specific metabolites as determined by Pearson pairwise correlation analysis. The blue columns represent the positive correlation pairs, and the orange ones represent the negative correlation pairs. Raw correlation coefficient values are labeled at each column as well listed in *SI Appendix*, Table S5. (*B*) Intrabacterial glutamine pool sizes, expressed as nanomoles per microgram residual peptide (*y* axis), after exposure of Mtb to a dose range of BDQ spanning 0–50× MIC or equimolar range of BDQi concentration. (*C*) Overlay plot of intrabacterial ATP and glutamine levels after exposure of Mtb to BDQ at 40× MIC over time (0 to 3 d); (*D*) Overlay plot of BDQ treatment on the EC of viable Mtb (left *y* axis) and in vitro activity of Mtb GlnA1 (right *y* axis) in the presence of the in vitro AXP ratio corresponding to the same range of BDQ concentrations. (*E*) Time course of de novo glutamine synthesis after 3-d preincubation of Mtb with BDQ (20× MIC), BDQi (same range as BDQ), or vehicle control (DMSO) followed by transfer to fresh media containing [15N] glutamate and metabolic profiling at the indicated points (0, 1, 2, and 3 h). (*F*) The EIC for [15N] glutamine ($m/z = 146.0589$ $[M\text{-}H]^-$), as in *E*. (*G*) CFU-based assay of Mtb viability after exposure of Mtb to the same range of BDQ or BDQi concentrations, as in *E*. All data points shown in *B–G* represent the average of 3 technical replicates and are representative of 2 independent experiments.

concentrations and ratios associated with the antimycobacterial activity of BDQ independent of substrate concentrations, demonstrating its intrinsic ability to directly sense and specifically respond, in part, to BDQ-mediated changes in AXP concentrations and energy charge in addition to its other well-known ATP-dependent regulation by posttranslational modification (26, 27). Moreover, isotopic labeling studies using $^{15}$N-labeled glutamate after a nonlethal 3-d preincubation of Mtb with BDQ revealed an almost complete cessation of glutamine biosynthesis (Fig. 2 *E*–*G*).

**Synergistic Effects of ATP Synthase and Glutamine Synthetase Inhibition on Mtb Viability.** Given the strong correlation between BDQ-mediated inhibition of ATP synthase and glutamine synthetase, and biphasic effect on glutamine levels, we tested the functional role of Mtb's GSs as indirect, but specific, secondary or downstream components of BDQ's bactericidal MoA. To do so, we first characterized the effect of methionine sulfoximine (MSO), a mechanism-based transition state inhibitor of all 4 Mtb GSs, on growth and synthesis of glutamine in Mtb (*SI Appendix*, Figs. S14 *A* and *C* and S15) (28, 29). Consistent with its in vitro activity (Fig. 3*A*), MSO inhibited Mtb growth in a dose-dependent manner that could be rescued by the addition of exogenous glutamine to the culture medium and was accompanied by parallel changes in intracellular glutamine pools (*SI Appendix*, Fig. S15). Based on this specificity, we evaluated the functional interaction between BDQ and MSO by checkerboard testing. Bliss independence modeling revealed a range of synergistic interactions that included a near 20-fold (17.78 ± 1.58) decrease in BDQ MIC at 0.25× MIC MSO (Fig. 3*B* and *SI Appendix*, Fig. S16 and Table S6), which was more potent than that reported for Btz043 (30, 31) (3.43 ± 0.37; Fig. 3*C* and *SI Appendix*, Table S6). This potentiation also manifested at the level of bacterial survival and was accompanied by a more rapid decrease in glutamine levels, supporting a specific and functional role for Mtb's GSs in the bactericidal activity of BDQ (Fig. 3 *D*–*F*). Checkerboard testing of BDQ and MSO further revealed that this synergy was not strictly dependent on glutamate and could be observed, albeit to a smaller degree, in an asparagine-based 7H9 media entirely lacking glutamate

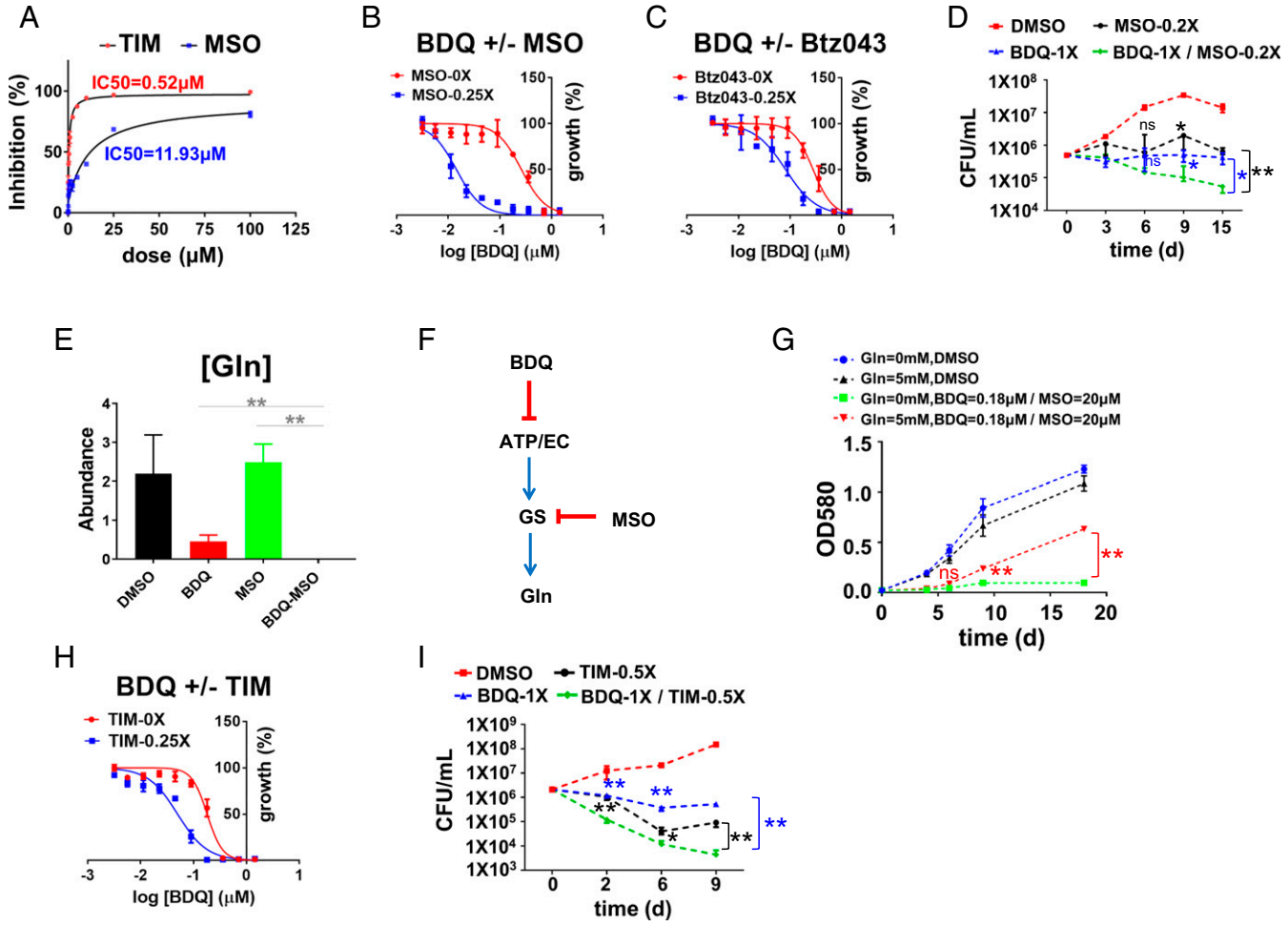


**Fig. 3.** Synergistic inhibition of Mtb viability and glutamine pools by BDQ and GS inhibitors. (*A*) In vitro inhibition curves and $IC_{50}$ values of Mtb GlnA1 by MSO (blue) and 2,4,5-TIM (red). (*B*, *C*, and *H*) Mtb growth inhibition curves of BDQ in the absence (red) and presence (blue) of varying concentrations of MSO (*B*, 0.25× MIC), Btz043 (*C*, 0.25× MIC), and TIM (*H*, 0.25× MIC). Curves depict $OD_{580}$ values after 10 d incubation in 7H9 liquid medium with 0.2% glucose and 0.2% glycerol as carbon sources and drugs, as indicated; the raw values of IC50 and ΔIC50 are listed in *SI Appendix*, Table S6. (*D*) CFU-based assay of Mtb viability after exposure to MSO (0.2× MIC), BDQ (1× MIC), or the combination. (*E*) Total bacterial glutamine pools after exposure of Mtb to BDQ (20× MIC), MSO (1× MIC), or the combination. $^{**}P < 0.01$ by unpaired Student *t* test. (*F*) Schematic depicting mechanism of synergy between BDQ and GS inhibitor, MSO. (*G*) Partial rescue of BDQ (0.18 μM)-MSO (20 μM) combination with exogenous (5 mM) glutamine. (*I*) CFU-based assay of Mtb viability after exposure to TIM (0.5× MIC), BDQ (1× MIC), or the combination. For *D*, *E*, *G*, and *I*, statistical differences were determined by unpaired *t* test. ns = not significant; $^{**}P < 0.01$; $^{*}0.01 < P < 0.05$. All data points shown in this figure represent the average of 3 technical replicates and are representative of 2 independent experiments. Error bars correspond to SEs of measurement.

(*SI Appendix*, Fig. S17 *A–E* and Table S6). Testing of 3 drug-sensitive clinical isolates from Haiti similarly confirmed that this synergy was not restricted to laboratory-adapted strains (*SI Appendix*, Fig. S18 *A–D* and Table S6).

Importantly, in all settings, we found that this potentiation could be selectively antagonized with the provision of exogenous glutamine, whereas glutamine did not measurably affect the antimycobacterial activity of BDQ alone (Fig. 3*G* and *SI Appendix*, Fig. S19). In contrast, no such potentiation was observed when BDQ was combined with *para*-aminosalicylic acid, a therapeutically validated metabolic inhibitor of Mtb's dihydropteroate synthase, the substrate of which was unaffected by BDQ (32) (*SI Appendix*, Fig. S20). The selective impact of exogenous glutamine on the activity of BDQ-GS inhibitor combinations thus provides further validation of GS as an essential, but downstream, indirect secondary target of BDQ.

To independently validate Mtb's GSs as a specific secondary or downstream component of BDQs bactericidal MoA, we tested a chemically and mechanistically unrelated inhibitor of Mtb's GlnA1 for similar effects. Previous work comparing the active site structures of Mtb GlnA1 and its human ortholog revealed a strong conservation of the amino acid binding site, where MSO binds, but substantial differences at the nucleotide binding pocket, prompting efforts to identify species-selective inhibitors targeting this site (33, 34). One such class of nanomolar inhibitors to emerge from these efforts are the 2,4,5-trisubstituted imidazoles (TIM) (35) (*SI Appendix*, Fig. S14 *B* and *C*). Consistent with published reports, we found that TIM inhibited purified recombinant Mtb GlnA1 with an $IC_{50}$ of 0.5 μM, and growth of Mtb with a MIC of 43 μM (Fig. 3*A* and *SI Appendix*, Fig. S21*A*). Metabolic profiling showed that that treatment of intact Mtb with antimycobacterial concentrations of TIM was accompanied by a matching depletion of glutamine pools (*SI Appendix*, Fig. S21*B*). Moreover, we observed that TIM potentiated BDQ, as reported both by MIC and the kinetics and extent of bacterial killing (Fig. 3 *H* and *I* and *SI Appendix*, Figs. S21*C* and S22 and Table S6). This potentiation was biochemically accompanied by an enhanced depletion of glutamine pools (*SI Appendix*, Fig. S21*D*) and could be selectively antagonized by exogenous glutamine (*SI Appendix*, Fig. S21*E*).

## Discussion

While challenging to interpret and exploit, MoA studies represent a conceptually rich but underappreciated route to rational drug development. Molecular technologies have helped facilitate the identification of individual targets for phenotypically active chemical compounds and biological phenotypes of interest. Their application in the design of drug combinations that are mechanistically rational, safe, and effective remains comparatively underexplored.

Drug phenotypes are complex or higher-order functions that, while experimentally well defined, correspond to the end product of a mechanistically complex sequence of events that is initiated by a discrete molecular interaction. This inciting interaction has formed the focus of most traditional drug development efforts and/or mechanism-of-action studies because of its direct chemical exploitability and the perceived lack of definable specificity in secondary or downstream MoA events. The latter view, however, has been recently challenged by the advent of systems-level technologies. With the discovery of highly specific systems-level readouts (or signatures) of drug activity, it has become possible to gain insight into specific primary and secondary readouts of drug activity. Moreover, such secondary or downstream MoA-related responses have increasingly made it possible to classify drug activity in the absence of specific knowledge of their targets.

We demonstrate here how these responses can also be leveraged for their information content as a window to mechanistically related targets. By seeking compound-, dose-, and time-dependent correlates of BDQ-mediated killing of Mtb during the prelethal phase of exposure, we were able to identify glutamine as a highly specific and essential indirect secondary biochemical target of BDQ from hundreds of annotated ATP-dependent reactions in the Mtb genome. That glutamine was unable to antagonize the activity of BDQ alone enabled us to further identify Mtb's GS as a critical collateral vulnerability rendered by BDQ, rather than a direct antimycobacterial target. Moreover, the ability of Mtb GS inhibitors to synergize with BDQ (as demonstrated by its ability to increase both the rate and extent of bacterial killing) reveals the potential of drug-induced collateral vulnerabilities (discussed here) to be exploited in the development of rational, mechanism-based drug combinations that, in the specific case of BDQ, may include helping to shorten its characteristic lag in onset of bactericidal activity. Our findings further indicate that, while the magnitude of synergy between BDQ and GS inhibition varies with the specific level of glutamate available to assimilate nitrogen, the fundamentally synergistic nature of this interaction remains intact even in the complete absence of glutamate in vitro. These results, in combination with the apparent essentiality of glutamine biosynthesis in vivo, support its potential therapeutic relevance to the broad and incompletely defined range of nutritional niches encountered by Mtb in the host during the course of infection (21, 22).

In 1952, Szybalski and Bryson first coined the term collateral sensitivity to describe a phenomenon in which an *E. coli* strain made resistant to 1 antibiotic exhibits hypersensitivity to a second mechanistically unrelated antibiotic compared with its drug-susceptible parent (36). Collateral sensitivity has subsequently been observed in drug-resistant cancer cells, and is believed to represent a form of synthetic lethality arising from the specific fitness costs imposed by a given form of drug resistance (37). Here, we reframe this same concept of fitness cost-induced synthetic lethality, but in this case imposed by drug-induced stress, rather than drug resistance, resulting in our use of the term collateral vulnerability, rather than sensitivity.

Recent evidence demonstrated that BDQ may also possess a chemical uncoupling activity that may contribute to both its bactericidal activity, when present at concentrations in excess of those required to achieve complete inhibition of ATP synthase activity, and its mechanism-based toxicity to host mitochondria (20, 38, 39). By focusing on downstream targets of its stereospecific activity against ATP synthase, our discovery of glutamine synthetase helps mitigate such concerns about this ambiguity and potential compound-specific toxicity.

That synergy between targets functioning in the same pathway can be exploited to clinically meaningful effect is well established, as exemplified by the efficacy of coformulated inhibitors of the de novo folate pathway in bacteria (40). The degree to which the specific synergy between BDQ and GS inhibition reported here can ultimately facilitate increased treatment efficacy, dose-sparing reductions in toxicity and decreased rates of drug resistance in vivo awaits the development of Mtb-specific GS inhibitors with pharmacokinetic exposures suitable for experimental testing. However, the attenuation of an Mtb *glnA1* deletion mutant and glutamine auxotroph in guinea pigs and mice supports the therapeutic potential of such an approach (22, 41). Interestingly, recent work identified an adaptive transcriptional response that mediated tolerance to BDQ and also included a key regulator of Mtb's glutamine synthetase (42). Awaiting the ability to test for in vivo synergy between BDQ and GS inhibitors, the concept that additional synergistic targets can be identified through similar MoA-directed studies represents a highly promising approach to engineering rational drug combinations with the potential to tackle the growing mismatch between antibiotic resistance and development.

## Materials and Methods

**Mtb Strains and Culture.** Mtb strain H37Rv and Haiti-17874, Haiti-19981, and Haiti-22897 were cultured in BSL3 at 37 °C in regular Middlebrook 7H9 broth,

non-Glu-7H9 broth (use same amount of Asn as the nitrogen source), or on 7H10 agar supplemented with 0.2% acetate (or 0.2% glucose, 0.2% glycerol, 0.2% propionate based on the experiment designs), 0.5 g/L Fraction V BSA, 0.04% Tyloxapol (7H9 broth only), and 0.085% NaCl. For metabolomics experiments, Mtb-inoculated filters were conducted according to previous literature (43).

**Synthesis of BDQ and BDQi.** Bedaquiline and its enantiomer were prepared according to literature (10), with minor modifications as described in *SI Appendix, SI Materials and Methods*.

**GS Inhibitors and $^{15}$N Labeling.** The TIM was provided by the Global Alliance for TB Drug Development. MSO was obtained from Sigma-Aldrich. $^{15}$N glutamate (NLM-135-1) was purchased from Cambridge Isotope Laboratories, Inc. For the isotopic labeling experiment, Mtb samples were first treated with DMSO, BDQ, or BDQi for 3 d. Afterward, filter-cultured bacteria were transferred to fresh 7H9 medium including DMSO/BDQ/BDQi and $^{15}$N glutamate (3.3 mM). Samples were collected at 0, 1, 2, and 3 h, and next analyzed by LC-MS method.

**MIC and CFU Assays.** Details are in *SI Appendix, SI Materials and Methods*.

**Drug Synergy Evaluation.** The protocol for generating the synergy-antagonism matrix was basically adapted from previous reports (44). Details are in *SI Appendix, SI Materials and Methods*.

**Metabolite Extraction and Liquid Chromatography-Mass Spectrometry.** Mtb metabolomes and LC-MS-based metabolomics analysis were conducted according to previous literature (43). Details are in *SI Appendix, SI Materials and Methods*. The concentrations of metabolites were calculated using residual protein abundance as the normalization factor. We also tried to use the total metabolites ion counts as the normalization factor, and these 2 methods generally show a similar pattern (*SI Appendix*, Fig. S23 *A* and *B*).

**Recombinant Mtb *GS* Expression, Purification, and Enzymatic Assays.** The plasmid pCR T7/CT-TOPO including the gene MtGS (GlnA1; Rv2220) was a kind gift from Sherry L. Mowbray (Uppsala University, Sweden). Protein expression and purification were as published previously (33). The details as well as the protocol of enzymatic assays are in *SI Appendix, SI Materials and Methods*.

**Bioinformatics Analysis and Data Visualization.** Details are in *SI Appendix, SI Materials and Methods*.

**ACKNOWLEDGMENTS.** We acknowledge funding support from the National Institutes of Health/National Institute of Allergy and Infectious Diseases (NIH/NIAID) Tuberculosis Research Unit (TBRU) (AI111143) and Bill and Melinda Gates TB Drug Accelerator (OPP1024050 to K.Y.R.). This work was also supported in part by funding by the Intramural Research Program of the NIAID/NIH (C.E.B. and H.I.M.B.). We thank Dr. Carl Nathan and all members of the K.Y.R. laboratory for critical discussions. We thank Dr. Sherry L. Mowbray for kindly providing the MtGS plasmid, Dr. Dirk Schnappinger and Dr. Sae Woong Park for kindly providing the script for computing antibiotic $IC_{50}$ values, Dr. Daniel Fitzgerald for kindly providing the Mtb isolates in Haiti, Mr. Michael Goodwin for help in NMR data collection, Ms. Yan Ling for help in protein purification, Ms. Xiuju Jiang for help in CFU assays, and Dr. Jun Zhang for help in figure preparation.

1. G. Chevereau, T. Bollenbach, Systematic discovery of drug interaction mechanisms. *Mol. Syst. Biol.* **11**, 807 (2015).
2. A. Zumla, P. Nahid, S. T. Cole, Advances in the development of new tuberculosis drugs and treatment regimens. *Nat. Rev. Drug Discov.* **12**, 388–404 (2013).
3. A. Koul, E. Arnoult, N. Lounis, J. Guillemont, K. Andries, The challenge of new drug discovery for tuberculosis. *Nature* **469**, 483–490 (2011).
4. H. Cho, T. Uehara, T. G. Bernhardt, Beta-lactam antibiotics induce a lethal malfunctioning of the bacterial cell wall synthesis machinery. *Cell* **159**, 1300–1311 (2014).
5. M. A. Lobritz *et al.*, Antibiotic efficacy is linked to bacterial cellular respiration. *Proc. Natl. Acad. Sci. U.S.A.* **112**, 8173–8180 (2015).
6. P. Belenky *et al.*, Bactericidal antibiotics induce toxic metabolic perturbations that lead to cellular damage. *Cell Rep.* **13**, 968–980 (2015).
7. M. Zampieri, M. Zimmermann, M. Claassen, U. Sauer, Nontargeted metabolomics reveals the multilevel response to antibiotic perturbations. *Cell Rep.* **19**, 1214–1228 (2017).
8. M. Zampieri *et al.*, High-throughput metabolomic analysis predicts mode of action of uncharacterized antimicrobial compounds. *Sci. Transl. Med.* **10**, 1–13 (2018).
9. K. Andries *et al.*, A diarylquinoline drug active on the ATP synthase of Mycobacterium tuberculosis. *Science* **307**, 223–227 (2005).
10. A. Koul *et al.*, Diarylquinolines target subunit c of mycobacterial ATP synthase. *Nat. Chem. Biol.* **3**, 323–324 (2007).
11. S. Joon *et al.*, The NMR solution structure of Mycobacterium tuberculosis F-ATP synthase subunit ε provides new insight into energy coupling inside the rotary engine. *FEBS J.* **285**, 1111–1128 (2018).
12. A. H. Diacon *et al.*, The diarylquinoline TMC207 for multidrug-resistant tuberculosis. *N. Engl. J. Med.* **360**, 2397–2405 (2009).
13. J. Cohen, Infectious disease. Approval of novel TB drug celebrated–with restraint. *Science* **339**, 130 (2013).
14. E. Pontali *et al.*, Cardiac safety of bedaquiline: A systematic and critical analysis of the evidence. *Eur. Respir. J.* **50**, 1701462 (2017).
15. A. Koul *et al.*, Delayed bactericidal response of Mycobacterium tuberculosis to bedaquiline involves remodelling of bacterial metabolism. *Nat. Commun.* **5**, 3369 (2014).
16. A. Koul *et al.*, Diarylquinolines are bactericidal for dormant mycobacteria as a result of disturbed ATP homeostasis. *J. Biol. Chem.* **283**, 25273–25280 (2008).
17. S. P. S. Rao, S. Alonso, L. Rand, T. Dick, K. Pethe, The protonmotive force is required for maintaining ATP homeostasis and viability of hypoxic, nonreplicating Mycobacterium tuberculosis. *Proc. Natl. Acad. Sci. U.S.A.* **105**, 11945–11950 (2008).
18. M. Gengenbacher, S. P. S. Rao, K. Pethe, T. Dick, Nutrient-starved, non-replicating Mycobacterium tuberculosis requires respiration, ATP synthase and isocitrate lyase for maintenance of ATP homeostasis and viability. *Microbiology* **156**, 81–87 (2010).
19. D. A. Lamprecht *et al.*, Turning the respiratory flexibility of Mycobacterium tuberculosis against itself. *Nat. Commun.* **7**, 12393 (2016).
20. M. Nandakumar, C. Nathan, K. Y. Rhee, Isocitrate lyase mediates broad antibiotic tolerance in Mycobacterium tuberculosis. *Nat. Commun.* **5**, 4306 (2014).
21. G. Harth, D. L. Clemens, M. A. Horwitz, Glutamine synthetase of Mycobacterium tuberculosis: Extracellular release and characterization of its enzymatic activity. *Proc. Natl. Acad. Sci. U.S.A.* **91**, 9342–9346 (1994).
22. M. V. Tullius, G. Harth, M. A. Horwitz, Glutamine synthetase GlnA1 is essential for growth of Mycobacterium tuberculosis in human THP-1 macrophages and Guinea pigs. *Infect. Immun.* **71**, 3927–3936 (2003).
23. L. Reitzer, Nitrogen assimilation and global regulation in Escherichia coli. *Annu. Rev. Microbiol.* **57**, 155–176 (2003).
24. S. T. Cole *et al.*, Deciphering the biology of Mycobacterium tuberculosis from the complete genome sequence. *Nature* **393**, 537–544 (1998).
25. D. E. Atkinson, The energy charge of the adenylate pool as a regulatory parameter. Interaction with feedback modifiers. *Biochemistry* **7**, 4030–4034 (1968).
26. B. M. Shapiro, E. R. Stadtman, The regulation of glutamine synthesis in microorganisms. *Annu. Rev. Microbiol.* **24**, 501–524 (1970).
27. A. Theron *et al.*, Differential inhibition of adenylylated and deadenylylated forms of M. tuberculosis glutamine synthetase as a drug discovery platform. *PLoS One* **12**, e0185068 (2017).
28. G. Harth, M. A. Horwitz, Inhibition of Mycobacterium tuberculosis glutamine synthetase as a novel antibiotic strategy against tuberculosis: Demonstration of efficacy in vivo. *Infect. Immun.* **71**, 456–464 (2003).
29. S. L. Mowbray, M. K. Kathiravan, A. A. Pandey, L. R. Odell, Inhibition of glutamine synthetase: A potential drug target in Mycobacterium tuberculosis. *Molecules* **19**, 13161–13176 (2014).
30. B. Lechartier, R. C. Hartkoorn, S. T. Cole, In vitro combination studies of benzothiazinone lead compound BTZ043 against Mycobacterium tuberculosis. *Antimicrob. Agents Chemother.* **56**, 5790–5793 (2012).
31. C. I. Bliss, The toxicity of poisons applied jointly. *Ann. Appl. Biol.* **26**, 585–615 (1939).
32. S. Chakraborty, K. Y. Rhee, Tuberculosis drug development: History and evolution of the mechanism-based paradigm. *Cold Spring Harb. Perspect. Med.* **5**, a021147 (2015).
33. W. W. Krajewski, T. A. Jones, S. L. Mowbray, Structure of Mycobacterium tuberculosis glutamine synthetase in complex with a transition-state mimic provides functional insights. *Proc. Natl. Acad. Sci. U.S.A.* **102**, 10499–10504 (2005).
34. W. W. Krajewski *et al.*, Crystal structures of mammalian glutamine synthetases illustrate substrate-induced conformational changes and provide opportunities for drug and herbicide design. *J. Mol. Biol.* **375**, 217–228 (2008).
35. J. Gising *et al.*, Trisubstituted imidazoles as Mycobacterium tuberculosis glutamine synthetase inhibitors. *J. Med. Chem.* **55**, 2894–2898 (2012).
36. W. Szybalski, V. Bryson, Genetic studies on microbial cross resistance to toxic agents. I. Cross resistance of Escherichia coli to fifteen antibiotics. *J. Bacteriol.* **64**, 489–499 (1952).
37. M. D. Hall, M. D. Handley, M. M. Gottesman, Is resistance useless? Multidrug resistance and collateral sensitivity. *Trends Pharmacol. Sci.* **30**, 546–556 (2009).
38. K. Hards *et al.*, Bactericidal mode of action of bedaquiline. *J. Antimicrob. Chemother.* **70**, 2028–2037 (2015).
39. K. Hards *et al.*, Ionophoric effects of the antitubercular drug bedaquiline. *Proc. Natl. Acad. Sci. U.S.A.* **115**, 7326–7331 (2018).
40. S. Chakraborty, T. Gruber, C. E. Barry, 3rd, H. I. Boshoff, K. Y. Rhee, Para-aminosalicylic acid acts as an alternative substrate of folate metabolism in Mycobacterium tuberculosis. *Science* **339**, 88–91 (2013).
41. S. Lee *et al.*, Protection elicited by two glutamine auxotrophs of Mycobacterium tuberculosis and in vivo growth phenotypes of the four unique glutamine synthetase mutants in a murine model. *Infect. Immun.* **74**, 6491–6495 (2006).
42. E. J. R. Peterson, S. Ma, D. R. Sherman, N. S. Baliga, Network analysis identifies Rv0324 and Rv0880 as regulators of bedaquiline tolerance in Mycobacterium tuberculosis. *Nat. Microbiol.* **1**, 16078 (2016).
43. M. Nandakumar, G. A. Prosser, L. P. de Carvalho, K. Rhee, Metabolomics of Mycobacterium tuberculosis. *Methods Mol. Biol.* **1285**, 105–115 (2015).
44. J. Lehár *et al.*, Synergistic drug combinations tend to improve therapeutically relevant selectivity. *Nat. Biotechnol.* **27**, 659–666 (2009).